IEEE Photonics Journal
An IEEE Photonics Society Publication

Open Access

Surface Passivation of Perovskite Film by Small Molecule Infiltration for Improved Efficiency of Perovskite Solar Cells

Volume 8, Number 5, October 2016

Ming Xu
Jing Feng
Xia-Li Ou
Zhen-Yu Zhang
Yi-Fan Zhang
Hai-Yu Wang
Hong-Bo Sun, ***Member, IEEE***

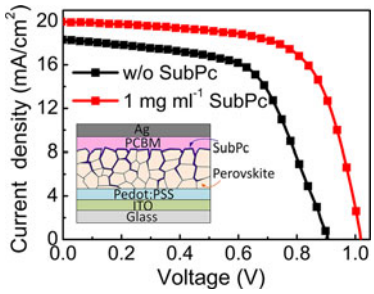

DOI: 10.1109/JPHOT.2016.2608619
1943-0655

Surface Passivation of Perovskite Film by Small Molecule Infiltration for Improved Efficiency of Perovskite Solar Cells

Ming Xu, Jing Feng, Xia-Li Ou, Zhen-Yu Zhang, Yi-Fan Zhang, Hai-Yu Wang, and Hong-Bo Sun, *Member, IEEE*

State Key Laboratory on Integrated Optoelectronics, College of Electronic Science and Engineering, Jilin University, Changchun 130012, China

DOI:10.1109/JPHOT.2016.2608619

Manuscript received July 8, 2016; revised September 1, 2016; accepted September 7, 2016. Date of publication September 13, 2016; date of current version September 28, 2016. This work was supported in part by the National 973 and in part by the NSFC programs under Grant 61322402, Grant 61590930, Grant 2013CBA01700, Grant 61505065, and Grant 61435005. Corresponding author: J. Feng (e-mail: jingfeng@jlu.edu.cn).

Abstract: Surface morphology of perovskite film is critical for highly efficient perovskite-based solar cells. The solution processed perovskite films tend to have voids and pin-holes between the crystals, which has been cited as very detrimental to device performance. The voids and pin-holes not only cause electrical shorting but deleteriously impact charge dissociation/transport/recombination because of the defects existed on the surface and grain boundaries of the perovskite films as well. Here, we demonstrate passivation of the perovskite surface and grain boundaries by small molecules through infiltration of subphthalocyanines (SubPc) into the perovskite film. Reduced surface defects have been obtained, which was verified by XRD and time-resolved dynamics measurements. As a result, the power conversion efficiency for the solution-processed planar heterojunction solar cells has been enhanced from 9.96% for the contrastive perovskite solar cells to 13.6% for the SubPc passivated perovskite solar cells.

Index Terms: Charge carrier lifetime, organic inorganic hybrid materials, photovoltaic cells, semiconductor devices.

1. Introduction

Optical solar cells are promising platforms for harvesting inexhaustible solar energy based on a variety of solar light absorbing materials, including crystalline silicon, thin-film polycrystalline or amorphous semiconductors; organic semiconductors and new materials are constantly emerging in this field [1]–[3]. Organic-inorganic hybrid perovskite materials as light harvesters in solid-state solar cells have gained intense attention in the past few years for their unique lattice structures and optoelectronic properties such as highly perfect crystalline structure, direct bandgap, large absorption coefficient, high charge carrier mobility and long charge carrier diffusion length [4]. Miyasaka *et al.* pioneered the first perovskite photovoltaic device in 2009, which exhibited power conversion efficiency (PCE) of 3.8% and they further improved the PCE over 9% [5], [6]. Over the past two years, average PCE of over 15% has been reported by different groups, and the highest efficiency of 22.1% has been achieved [7]. The rapid rise in PCE has made perovskite-based solid-state solar cells a highly promising commercial technology for solar energy conversion.

The semiconductor perovskite materials exhibit ambipolar transport properties, allowing them to transport both hole and electron simultaneously in hybrid solar cells [8]. The long charge carrier diffusion lengths of perovskite materials (1 μm in $CH_3NH_3PbI_{3-x}Cl_x$ and 100 nm in $CH_3NH_3PbI_3$) [9] encourage the progressive development of planar heterojunction (PHJ) perovskite solar cells. In contrast to perovskite materials infiltrated in mesoporous metal oxide scaffolds [10], the PHJ structure is compatible with solution-processing techniques and would enable its flexible device application due to the low temperature fabrication processes [11]. One of the main challenges encountered in the PHJ perovskite solar cells is how to optimize film morphology. It has been proposed that the limited performance of the PHJ architecture may arise from pin-hole and voids formation [12]. Trap-states localized at the surface and grain boundaries of the perovskite film will induce mono-molecular recombination mode [13]. Moreover, the incomplete coverage of the perovskite results in low-resistance shunting paths and lost light absorption in the solar cells. Many efforts have been made to solve this problem by optimizing the quality of the perovskite crystal to increase grain size and decrease the voids, such as two-step iodide deposition [14], two-source thermal evaporation [15], and vapor-assisted solution process [16]. On the other hand, Huang *et al.* reported that the trap states can be passivated by spin-coating fullerene onto the perovskites, which provide another direction to enhance the device efficiency by film morphology modification [17].

In this paper we employed a small molecule of boron subphthalocyanine chloride (SubPc) to passivate the defects. We found that filling up the voids and pin-holes is easier due to its lower viscosity of the small molecule compared to that of the polymer. Moreover, compared to the polymer passivation, thermal annealing is avoided for the spin-coated SubPc film, which eliminated the possible damage to the perovskite by the further thermal annealing. We observed that free charge carrier lifetime was increased, which indicated effective passivation of the surface defect trap-states [18], [19]. The SubPc passivation results in an improved device performance of the perovskite solar cells, and the PCE has enhanced from 9.96% for the contrastive perovskite solar cells to 13.6% for the SubPc passivated perovskite solar cells

2. Fabrication and Characterization

All the chemicals were used as received, including CH_3NH_3I (99.999%, Xi'an polymer light technology corp.), PEDOT: PSS (Clevious), $PbCl_2$ (99.999%, Lumtec), PCBM and SubPc (Lumtec). For the non-stoichiometric perovskite precursor solution, a 1: 3 molar ratio of $PbCl_2/CH_3NH_3I$ was mixed in anhydrous N, N-Dimethylformamide (DMF), with final concentrations 0.8 M lead chloride and 2.4 M methylammonium iodide. The solution is stored under a dry nitrogen atmosphere while stirring overnight before use.

PEDOT: PSS was spin coated onto a clean ITO surface under 4000 rpm and then annealed at 120 °C for 15 min. The precursor solution was spin-coated onto the PEDOT: PSS layer at 5000 rpm and then annealed at 100 °C for 2 h. After that, SubPc in toluene solution was spin-coated onto the crystallization perovskite film for perovskite passivation. 2 wt% PCBM in chloroform solution was coated subsequently at 1500 rpm. Above steps were operated in the nitrogen environment. Finally, the device was transferred to a vacuum chamber for Ag electrode deposition. The device area is 0.04 cm^2. The characteristics of all the devices in our experiment were tested in air without any encapsulation. The thickness of cathode layer was monitored by quartz crystals, and calibrated by a Spectroscopic Ellipsometers (J. A. Woollam Co., Inc., USA). The SEM images were taken on a JEOL JSM-7500F. The X-ray diffraction patterns were collected on a Rigaku X-ray powder diffractometer using CuK ⟨alpha⟩ radiation ($\lambda = 1.54050$ A). The absorption spectra of the samples were measured by a UV-vis spectrophotometer (UV-2550, Shimadzu Co., Inc., Japan). The current density-voltage (J-V) characteristics of all the solar cells were measured using a Keithley 2400 source measure unit under a 1 sun simulated AM 1.5G illumination. With an AAA class solar simulator (XES-70S1, san ei electric co.), the light intensity with 100 mW cm^{-2} was calibrated by standard Si photodiode detector equipped with a KG-5 filter. External quantum efficiencies were measured by an Enli Technology (Taiwan) EQE measurement system. The results given in the paper

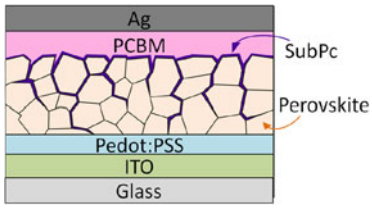

Fig. 1. Schematic diagram of SubPc passivated perovskite solar cells.

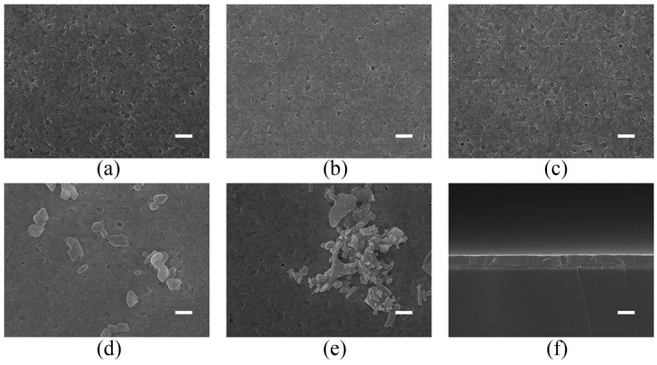

Fig. 2. SEM images of the non-passivated perovskite film (a) and SubPc passivated perovskite films with various SubPc concentrations of 0.5 mg ml^{-1} (b), 1 mg ml^{-1} (c), 2 mg ml^{-1} (d), and 5 mg ml^{-1} (e). (f) Cross-sectional view of the SubPc passivated perovskite film with the concentration of 1 mg ml^{-1}. The scale bar is 1 μm.

are the average values. TA spectroscopy were obtained by femtosecond time-resolved pump-probe technology and the carrier dynamic traces were obtained by controlling the relative delay between the pump and the probe pulses with a stepper-motor-driven optical delay line.

3. Results and Discussions

3.1. Morphology Analysis

Small molecule of SubPc as excellent light absorption and charge transport material has unusual optical and electrical properties and render itself to the potential materials for photovoltaic and high-density optical data storage devices and nano-technological applications [20]. The perovskite film with SubPc passivation is shown in Fig. 1. The voids and pinholes existed in perovskite film are infiltrated by the SubPc and the film surface is coated by the SubPc solution. Top view SEM images were conducted to inspect the morphology of the perovskite films with and without the SubPc passivation. As shown in Fig. 2, SubPc with low concentration has obvious infiltrated into the perovskite film without apparent change of the surface morphology compared with the reference. When the concentration was increased, the small molecule aggregated into clusters at the perovskite surface which has a negative influence on charge performance of the perovskite solar cells. Therefore, the low concentration between 0.5 and 1 mg ml^{-1} was better adopted in perovskite solar cells. Sectional view SEM image (Fig. 2f) illustrates that 1 mg ml^{-1} SubPc was infiltrated into contrastive perovskite film without any molecule aggregation. Meanwhile the sectional view has affirmed about 300 nm thickness of the perovskite film.

3.2. Characterizations

The steady-state absorption spectra of the perovskite films without or with various concentrations of SubPc passivation was exhibited in Fig. 3. The steady absorption spectra of $CH_3NH_3PbI_{3-x}Cl_x$

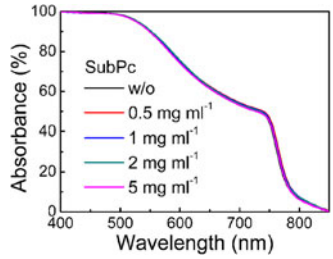

Fig. 3. UV/vis absorption spectra of the non-passivated and SubPc passivated perovskite films with various concentrations.

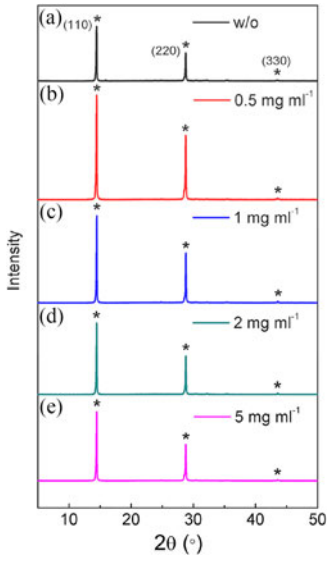

Fig. 4. XRD spectra of the non-passivated (a) and SubPc passivated perovskite films with various SubPc concentrations of 0.5 mg ml^{-1} (b), 1 mg ml^{-1} (c), 2 mg ml^{-1} (d), and 5 mg ml^{-1}(e).

scanning from ultraviolet to near infrared regime exhibits two distinct shoulders located at ~480 and ~750 nm. The absorption shoulder at ~750 nm is attributed to the direct gap transition from the first valence band maximum to the conduction band minimum. The absorption shoulder at ~480 nm is considered as the residue in the partial decomposed process [21]. The SubPc passivation films with various concentrations show the same absorption characteristics compared with the reference. Moreover, the absorption peak of SubPc (~590 nm) [22] is not observed in the spectra, which indicates that the small amount of the SubPc has no influence on the absorption of the perovskite film.

X-ray diffraction (XRD) was analyzed to assess the impact of infiltrated SubPc on the crystallization of perovskite film. Fig. 4 presents XRD patterns of the contrastive and SubPc-passivated $CH_3NH_3PbI_{3-x}Cl_x$ films with various concentrations. The main diffraction peaks at 14.2°, 28.5° and 43.3° are assigned to the lattice orientation (110), (220) and (330) of the mixed-halide perovskite with an orthorhombic crystal structure, respectively [23]. The perovskite films presented here are pure phase, crystallized in the expected tetragonal I4/mcm space group. No impurities can be observed and all samples crystallize with similar lattice parameters. The peak intensity of the passivated film with low concentration SubPc has been increased obviously, which might be attributed to a reduced surface defect and improved film quality induced by the small molecule passivation.

Further investigation of the effect of small molecule passivation on the film quality was performed through studying the fundamental photophysics of the reference and SubPc-passivated

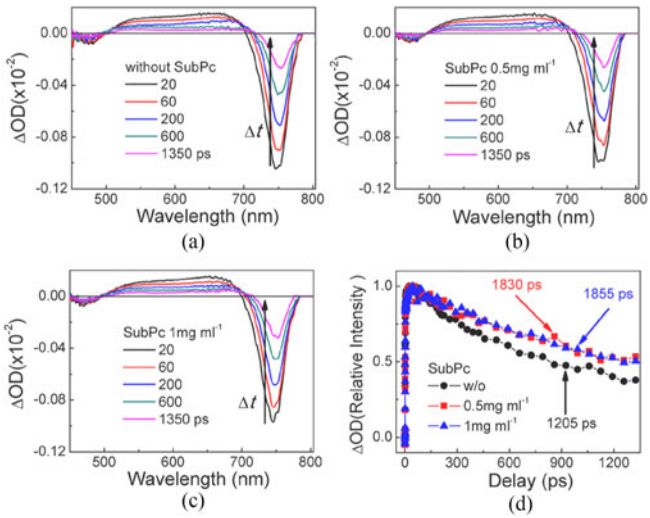

Fig. 5. Time-resolved pump-probe measurement for non-passivated perovskite (a) and SubPc passivated perovskite solar cells with concentrations of 0.5 mg ml^{-1} (b) and 1 mg ml^{-1} (c). (d) Decay kinetics examine the related band edge bleaching at the bandgap.

$CH_3NH_3PbI_{3-x}Cl_x$ perovskite films by transient absorption (TA) technology. As shown in Fig. 5(a)–(c), the TA spectra (pumped under 400 nm with intensity of 7.6 μJ cm^{-2}) obviously shows two ground bleaching signals at 754 nm ($\sim$1.621 eV, band gap transition) and 485 nm (2.557 eV, trap-states photobleaching), as well as the broad excited-state absorption from 500 to 700 nm. The arrow indicates the direction of ground state bleach recovery. These transient signals are caused by photobleaching, and both shape and intensity of all the spectra signals are independent of the concentration of the SubPc. The relation of the time resolved difference TA spectra could last for a timescale of nanoseconds, which indicates the free charge carrier recombination [24]. The TA spectra illustrate that the absorption properties of the perovskite films are not affected by the introduction of the SubPc, which is consistent with that of the measured absorption spectra (see Fig. 3). To further verify the effect of the SubPc passivation, we focused on the 754 nm photoinduced bleach singal to probe the band-edge charge carrier dynamics in the $CH_3NH_3PbI_{3-x}Cl_x$ films. Fig. 5(d) displays the carrier recombination dynamics of contrastive and SubPc-passivated perovskite films with concentration of 0.5 mg ml^{-1} and 1 mg ml^{-1} under the identical pump intensity. The kinetic decay rates of band-edge at $\sim$754 nm become slower in the SubPc-passivated perovskite films. The lifetime of the contrastive perovskite film is 1205 ps, while it is increased to 1830 ps (0.5 mg ml^{-1}) and 1850 ps (1 mg ml^{-1}), respectively, for the passivated films. Therefore, the SubPc passivation has the effect to increase the lifetime of the perovskite film due to the defect passivation of the SubPc on the grain boundaries and surface of the perovskite film. The increased lifetime means prolonged carrier diffusion length, which would be a great benefit to the device performance of the perovskite solar cells.

3.3. Photovoltaic Performance

The passivation effect of the SubPc on the device performance has been examined by comparing the J-V and EQE characteristics of the perovskite solar cells with and without the SubPc passivation and is shown in Fig. 6. The detailed solar cell performance parameters are summarized in Table 1. Obvious improvement of the device performance can be observed from the passivated devices. The reference cell without the passivation shows Voc, Jsc, and FF of 0.9 V, 18.3 mA cm^{-2}, and 60.16%, respectively, leading to a PCE of 9.96%. In the case of the passivated devices, the performance was obtained for the device with the SubPc concentration of 1mg ml^{-1}, which exhibits a PCE of 13.6%, with Voc of 1.02 V, Jsc of 19.94 mA cm^{-2}, and FF of 66.72%, respectively. The defect passivation

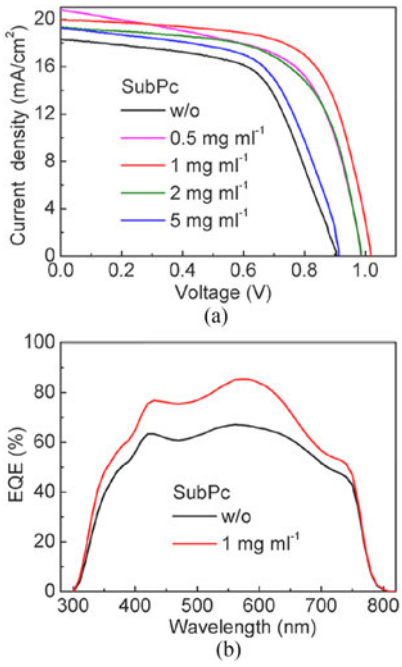

Fig. 6. J-V (a) and EQE (b) of the non-passivated and SubPc passivated perovskite solar cells.

TABLE 1
Photovoltaic Parameters of Perovskite Solar Cells Without and With Subpc Passivation

Concentration of SubPc (mg ml^{-1})	Voc (V)	Jsc (mA cm^{-2})	FF (%)	PCE (%)
w/o	0.90	18.31	60.16	9.96
0.5	0.99	20.79	60.06	12.34
1	1.02	19.94	66.72	13.60
2	0.99	19.29	62.90	12.01
5	0.91	19.26	60.72	10.66

effectively suppresses the charge recombination and longer carrier diffusion length, which contributes to the enhanced cell performance, especially enhanced Jsc and FF. This is further supported by the decreased series resistance of 133 Ω cm^2 and the corresponding shunt resistance of 28.2 kΩ cm^2 after 1 mg ml^{-1} SubPc passivation. However, the series resistance of reference cell without the passivation is 179 Ω cm^2, and corresponding shunt resistance is 27.1 kΩ cm^2. The SubPc infiltration of the pinhole and voids in perovskite film to reduce the leakage current also contributes to the enhanced FF and Voc. It is identified that Voc increases with the concentration of SubPc from 0.5 to 2 mg ml^{-1} and then severely decreases with further increased SubPc concentration. The SubPc aggregation into clusters at high concentration would hinder the electron transfer from the perovskite layer to PCBM layer, which leads to the degradation of the device performance. The external quantum efficiency (EQE) spectrum of the solar cells without or with SubPc at the concentration of 1 mg ml^{-1} exhibits an obvious enhancement in the wide spectral response from 400 nm to 800 nm.

4. Conclusion

In conclusion, we have demonstrated passivation of the perovskite film by employing small molecule infiltration. The small molecule of SubPc has infiltrated into the voids and pinholes of the perovskite film to realize a defect passivation at the perovskite surface and grain boundaries. The defect passivation results in an increased carrier lifetime, which contributes to improved device efficiency. The power conversion efficiency for the solution-processed planar heterojunction solar cells has been enhanced from 9.96% for the non-passivated perovskite solar cells to 13.6% for the SubPc passivated perovskite solar cells. Different from the methods of improving the quality of perovskite crystal in the process of crystallization, the passivation method provides a simple and low-cost avenue to improve the quality of the perovskite film and further increase its efficiency. This work may open a door for deeper optimization of perovskite films applied for a range of optical and optoelectronic devices.

References

[1] Z. C. Holman, S. De Wolf, and C. Ballif, "Improving metal reflectors by suppressing surface plasmon polaritons: A priori calculation of the internal reflectance of a solar cell," *Light Sci. Appl.*, vol. 2, no. 10, Jul. 2013, Art. no. e106.

[2] Y. Jin *et al.*, "Improved performance of ITO-free organic solar cells using a low-workfunction and periodically corrugated metallic cathode," *IEEE Photon. J.*, vol. 4, no. 5, pp. 1737–1743, Oct. 2012.

[3] K. T. Lee, J. Y. Lee, S. Seo, and L. Guo, "Colored ultrathin hybrid photovoltaics with high quantum efficiency," *Light Sci. Appl.*, vol. 3, Aug. 2014, Art. no. e215.

[4] D. Shi *et al.*, "Low trap-state density and long carrier diffusion in organolead trihalide perovskite single crystals," *Science*, vol. 347, no. 6221, pp. 519–522, Jan. 2015.

[5] A. Kojima, K. Teshima, Y. Shirai, and T. Miyasaka, "Organometal halide perovskites as visible-light sensitizers for photovoltaic cells," *J. Amer. Chem. Soc.*, vol. 131, no. 17, pp. 6050–6051, Apr. 2009.

[6] H. S. Kim *et al.*, "Lead iodide perovskite sensitized all-solid-state submicron thin film mesoscopic solar cell with efficiency exceeding 9%," *Sci. Rep.*, vol. 2, Aug. 2012, Art. no. 591.

[7] NREL chart, [Online]. Available: http://www.nrel.gov/ncpv/images/efficiency_chart.jpg

[8] W. S. Yang *et al.*, "High performance photovoltaic perovskite layers fabricated through intramolecular exchange," *Science*, vol. 348, no. 6240, pp. 1234–1237, Jun. 2015.

[9] S. D. Stranks *et al.*, "Electron-hole diffusion lengths exceeding 1 micrometer in an organometal trihalide perovskite absorber," *Science*, vol. 342, no. 6156, pp. 341–344, Oct. 2013.

[10] J. M. Ball, M. M. Lee, A. Hey, and H. J. Snaith, "Low-temperature processed meso-superstructured to thin-film perovskite solar cells," *Energy Environ. Sci.*, vol. 6, pp. 1739–1743, 2013.

[11] D. Liu and T. L. Kelly, "Perovskite solar cells with a planar heterojunction structure prepared using room-temperature solution processing techniques," *Nat. Photon.*, vol. 8, no. 2, pp. 133–138, Feb. 2014.

[12] P. W. Liang *et al.*, "Additive enhanced crystallization of solution-processed perovskite for highly efficient planar-heterojunction solar cells," *Adv. Mater.*, vol. 26, no. 22, pp. 3748–3754, Jun. 2014.

[13] Z. Y. Zhang *et al.*, "Elucidating the band structure and free charge carrier dynamics of pure and impurities doped CH3NH3PbI3-xClx perovskite thin films," *Phys. Chem. Chem. Phys.*, vol. 17, pp. 30084–30089, Sep. 2015.

[14] J. Burschka *et al.*, "Sequential deposition as a route to high-performance perovskite-sensitized solar cells," *Nature*, vol. 499, no. 7458, pp. 316–319, Jul. 2013.

[15] M. Liu, M. B. Johnston, and H. J. Snaith, "Efficient planar heterojunction perovskite solar cells by vapour deposition," *Nature*, vol. 501, no. 7467, pp. 395–398, Sep. 2013.

[16] Q. Chen *et al.*, "Planar heterojunction perovskite solar cells via vapor-assisted solution process," *J. Amer. Chem. Soc.*, vol. 136, no. 2, pp. 622–625, Dec. 2014.

[17] Y. C. Shao, Z. G. Xiao, C. Bi, Y. B. Yuan, and J. S. Huang, "Origin and elimination of photocurrent hysteresis by fullerene passivation in CH3NH3PbI3 planar heterojunction solar cells," *Nat. Commun.*, vol. 5, Dec. 2014, Art. no. 5784.

[18] Z. G. Xiao *et al.*, "Efficient, high yield perovskite photovoltaic devices grown by interdiffusion of solution-processed precursor stacking layers," *Energy Environ. Sci.*, vol. 7, pp. 2619–2623, May 2014.

[19] T. Leijtens, G. E. Eperon, S. Pathak, A. Abate, M. M. Lee, and H. J. Snaith, "Overcoming ultraviolet light instability of sensitized TiO2 with meso-superstructured organometal tri-halide perovskite solar cells," *Nat. Commun.*, vol. 4, Dec. 2013, Art. no. 2885.

[20] Y. F. Liu *et al.*, "Highly flexible inverted organic solar cells with improved performance by using an ultrasmooth Ag cathode," *Appl. Phys. Lett.*, vol. 101, no. 13, Sep. 2012, Art. no. 133303.

[21] G. Xing *et al.*, "Long-range balanced electron- and hole-transport lengths in organic-inorganic CH3NH3PbI3," *Science*, vol. 342, no. 6156, pp. 344–347, Oct. 2013.

[22] Y. G. Bi *et al.*, "Dual-periodic-corrugation-induced broadband light absorption enhancement in organic solar cells," *Organ. Electron.*, vol. 27, Dec. 2015, Art. no. 167.

[23] M. M. Lee, J. Teuscher, T. Miyasaka, T. N. Murakami, and H. J. Snaith, "Efficient hybrid solar cells based on meso-superstructured organometal halide perovskites," *Science*, vol. 338, no. 6107, pp. 643–647, Oct. 2012.

[24] J. S. Manser and P. V. Kamat, "Band filling with free charge carriers in organometal halide perovskites," *Nat. Photon.*, vol. 8, no. 9, pp. 737–743, Aug. 2014.